VERTICAL POSITION CONTROL ON COMPASS-D

TOKAMAK CONTROL

KEYWORDS: *tokamak, vertical position control*

PARAG VYAS*† and DENIS MUSTAFA *University of Oxford*
Department of Engineering Science, Parks Road, Oxford OX1 3PJ, United Kingdom

A. WILLIAM MORRIS *UKAEA Fusion, Culham, Abingdon*
Oxfordshire OX14 3DB, United Kingdom

Received August 9, 1995
Accepted for Publication August 18, 1997

Theoretical and experimental work on the vertical position control system on the COMPASS-D tokamak is described. An analog proportional + derivative (P + D) system is currently used, and two important sources of disturbance are observed in the system. One source is 600-Hz noise from thyristor power supplies, and the other is impulselike disturbances due to edge-localized modes (ELMs). A high-order controller is developed using the $\mathcal{H}_\infty$ technique to reduce the effect of the 600-Hz noise. This initial design is based on a model of the plasma position system obtained from system identification. The controller is implemented on a digital signal processor and tested on COMPASS-D. The controller synthesis procedure and the experimental results are presented. Large, separated ELMs on COMPASS-D cause impulselike responses to be observed in the power amplifier and position signals. Closed formulas are given for the minimum possible peak of the impulse response of the system, which is used to find the limit of performance.

INTRODUCTION

Large tokamaks such as the Joint European Torus (JET) and the International Thermonuclear Experimental Reactor (ITER) operate single-null diverted (SND) plasmas which are vertically unstable. COMPASS-D is a small tokamak that also operates with SND plasmas, and we present experimental and theoretical work on its vertical position control system. There are two important sources of disturbance on COMPASS-D. One source is 600-Hz noise from thyristor power supplies, and the other is impulselike disturbances due to edge-localized modes (ELMs). In this paper, separate control strategies are presented to deal with each of these.

An overview of the current analog proportional + derivative (P + D) vertical position control system is first given. Then we describe the design of controllers using the $\mathcal{H}_\infty$ control theory[1] to reduce the 600-Hz noise. These controllers have been tested with a digital signal processor (DSP) system on COMPASS-D, and preliminary experimental results are presented.

ELMs are plasma instabilities that are often observed on COMPASS-D, and large, separated ELMs add an impulselike disturbance to the system. This type of ELM causes large excursions in the plasma position and requires a large peak response from the controlling amplifier. Saturation of the amplifier, leading to vertical disruptions, is sometimes observed. The problem of minimizing the peak of the response to a fixed input has been solved by Dahleh and Pearson.[2] The result involves solving a linear programming problem with an infinite number of constraints. For COMPASS-D and an impulse model of ELMs, we obtain analytical results that allow us to examine the limits of performance.

For the position control experiments, COMPASS-D typically operated with SND plasmas, with plasma current $I_p \approx 150$ kA, major radius $R_p \approx 0.56$ m, minor radius $a \approx 0.18$ m, and elongation $\kappa \approx 1.6$. The vacuum vessel wall is made from 3-mm-thick Inconel, and the time constant for the penetration of the radial field, which is used for vertical position control, through the vacuum vessel is estimated to be in the range of 420 to 470 μs. The plasma shape and vessel geometry are similar to the ITER design, and phenomena such as ELMs are also expected to be present on ITER. For more details about COMPASS-D see Ref. 3, and for modeling details see Refs. 4 and 5.

*Current address: CRPP-EPFL, 1015 Lausanne, Switzerland.
†E-mail: Parag.Vyas@epfl.ch

PRESENT CONTROL SYSTEM

The control loops for the plasma shape, radial position, and vertical position are decoupled on COMPASS-D in that different poloidal field coils and control loops are used for each system. The coils in each loop are chosen to reduce the interaction with other loops. The vertical position system uses antiparallel coils connected in series ($L = 94.8\ \mu$H and $R = 11.5\ \text{m}\Omega$) above and below the vessel to generate the radial field required for vertical position control (Fig. 1). The coils are powered by one or sometimes two 250-kW (± 50 V, ± 5 kA) transistor amplifiers (6-kHz bandwidth).

Figure 2 contains a diagram of the system showing that the proportional and derivative signals are obtained from two different sources. The position signal is obtained by summing and then integrating the signals from four flux loops (FLs) outside the vessel, and the velocity signal is the sum of eight internal partial Rogowski (IPR) coils inside the vessel. The flux loop coils provide a position signal close to that obtained from poloidal field reconstructions and, unlike the IPR coils, are not sensitive to helical modes and do not contain a large level of high-frequency noise. However the flux loop coils are shielded by the vessel wall. The two signals are designed to provide position measurements of the current centroid and work remarkably well when compared with the current centroid position obtained from poloidal field reconstructions (Fig. 3). The current centroid position is controlled rather than the plasma boundary because a separate system controls the plasma shape. A reference position signal is used to set the position, and multiplying waveform generators are used to adjust the proportional and derivative gains. The gains have been optimized empirically; i.e., they were scanned until suitable experimental performance was obtained.

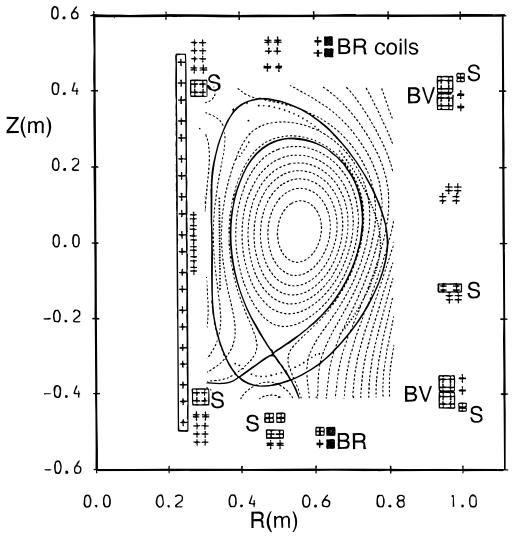

Fig. 1. COMPASS-D vessel, location of control coils, and SND plasma: vertical position control coils (BR), radial position coils (BV), shaping coils (S).

The system satisfactorily stabilizes plasmas with instability growth rates of up to $\sim 2500\ \text{s}^{-1}$. However, noise is present from coupling to thyristor power supplies generating 600-Hz and higher harmonics. The effect of the 600-Hz oscillation on the plasma position is small ($<$1-mm amplitude), but large voltage swings are present at the amplifier output ($\sim$20-V amplitude). Saturation of the amplifier can sometimes occur and can lead to loss of control and disruptions. A P + D controller based on signals from only the flux loops has also been tested and found to be not as reliable as the current system, which can be explained by the effect of the vessel wall in shielding the flux loop coils from plasma motion. System identification of models of the plasma response with external and internal coils shows that shielding by the vessel wall reduces the control stability margin.[4]

DSP CONTROLLER DESIGN

A DSP system was installed to improve the performance of the control system. The hardware consists of an AT&T DSP32C (up to 25 Mflops, 32-bit floating point), two analog-to-digital converters and two digital-to-analog converters (16-bit resolution, up to 200-kHz sampling frequency). The objectives of the controller are to

1. stabilize the plasma during startup and flattop
2. avoid coupling to helical magnetohydrodynamic (MHD) modes
3. reduce the amplitude of the 600-Hz component
4. regulate the plasma position, allowing only small deviations from the reference position.

To avoid coupling to helical MHD modes it was decided to use only the flux loop position signal and not the IPR velocity signal. This also simplifies the controller design and makes the results more relevant to the ITER scenario, where there may not be any internal magnetic pickup coils close to the plasma. A sampling frequency of 20 kHz was chosen because this greatly exceeds the bandwidth of the system but is well within the computational speed and numerical accuracy limits of the DSP.

An open-loop model of the COMPASS-D system was obtained for controller design purposes. The plasma position system was modeled using system identification, which is the process of fitting the coefficients of mathematical models to experimental data. Experiments were performed in which the position reference signal was switched at random between two levels at intervals of 100 μs (Ref. 5). This was done to excite the modes of the plasma position system, which responded with a maximum of 1-cm peak-to-peak excursions in the plasma

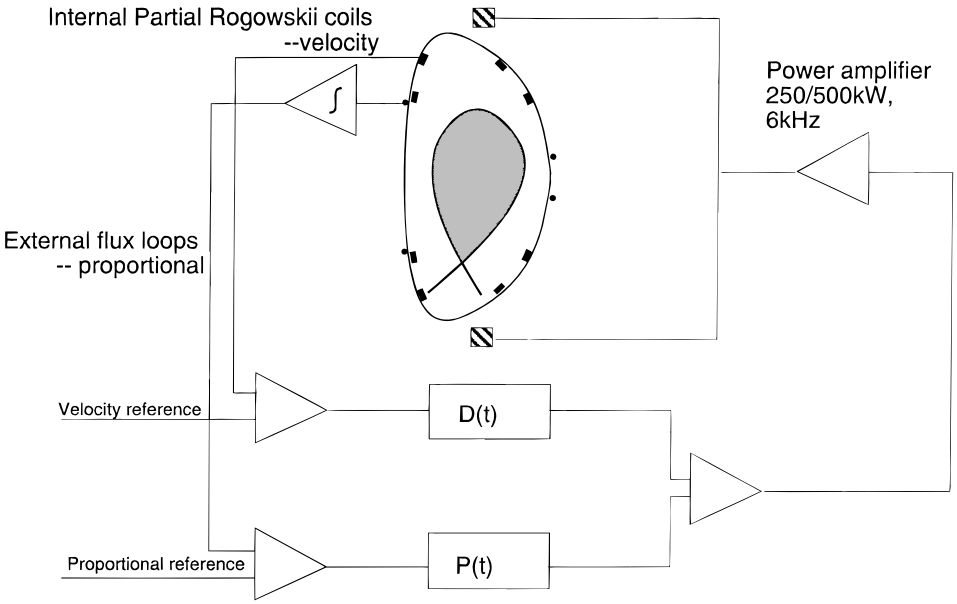

Fig. 2. Schematic of vertical position control loop.

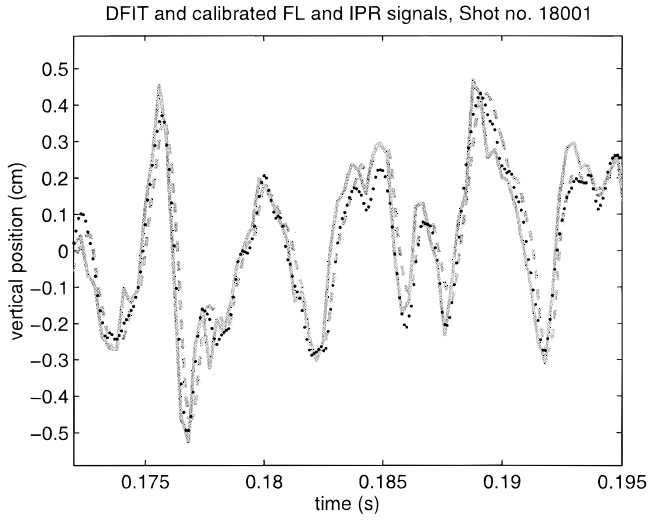

Fig. 3. Comparison of vertical position signals: current centroid from poloidal field reconstructions (solid), calibrated flux loop signal (dash), and integrated and calibrated IPR signal (dot).

position. After anti-alias filtering, the position and amplifier signals were sampled at 20 kHz. The input and output data were then notch filtered to remove the 600-Hz noise and high-pass filtered with cutoff at 100 Hz to emphasize the high-frequency components. At each sample instant i (sampling frequency 20 kHz), the response of the flux loop plasma position y_i (in volts) can be related to the amplifier current u_i using the discrete time difference equation

$$y_i = b_1 u_{i-1} + b_2 u_{i-2} - a_1 y_{i-1} - a_2 y_{i-2} - a_3 y_{i-3} \ .$$

The coefficients a_k and b_k can be calculated from a least-squares fit to the experimental data. The model can be converted to a continuous time differential equation using Tustin's approximation, and taking the Laplace transform gives the continuous time transfer function.

A discrete time model from coil current to flux loop position signal for a typical shot ($I_p = 150$ kA and $\kappa = 1.6$) was obtained using system identification. The resulting continuous time transfer function from control coil current to flux loop position signal was

$$P_{\mathrm{FL}}(s) = 1.1651 \times 10^{-5} \times \frac{(s + 41\,164)(s + 40\,000)(s - 40\,000)}{(s + 51\,136)(s + 6704)(s - 2260)} \ ,$$

where s is the Laplace transform variable in the complex frequency domain $s = \sigma + j\omega$. There is one unstable pole at $s = 2260\ \mathrm{s}^{-1}$, representing the vertical instability growth rate, and two other stable poles, modeling the stable dynamics of the plasma and the sample delay.

The power supply and control coil model from control signal voltage to amplifier output current was

$$P_c(s) = \frac{K_a}{(L_c\, s + R_c)} \ ,$$

where $K_a = -57.6$ represented the power supply gain, and the control coil (including leads) self-inductance and resistance were approximated as $L_c = 100\ \mu$H and $R_c = 10\ \mathrm{m}\Omega$, respectively. The model of the COMPASS-D plant consists of the two components connected in series

$$P(s) = P_c P_{\mathrm{FL}} \ .$$

During the startup, major changes in the plasma vertical position system occur, including changing from stable to unstable as the plasma shape changes from circular to SND. System identification was used on shots with plasmas at different elongations (Fig. 4). The magnitude of the plasma unstable pole, effectively the plasma response bandwidth, increases with elongation, and the D.C. gain of the model decreases. There is no discernible trend in the values of the other poles or the zeros in the models.

Initial controllers designed using a direct digital implementation of a P + D controller had the problem of poor stability margins and were unable to stabilize a normal plasma. This is also true of flux-loop-only analog P + D controllers, which have also been tested in the past. Plasma position controllers based on the $\mathcal{H}_\infty$ design method have been proposed (see Refs. 6 and 7), and this method was investigated on COMPASS-D.

Simple P + D controllers have an advantage in that they are easily implemented and require only two coefficients to be determined. High-order controllers offer more flexibility but are more difficult to design because more coefficients must be determined. The $\mathcal{H}_\infty$ technique allows constraints to be specified on the desired closed-loop response of the system, and, given a model of the plant $P(s)$, a controller $C(s)$ is calculated that satisfies the closed-loop constraints. The constraints are specified to limit the $\mathcal{H}_\infty$ norm of the closed-loop frequency response. For a transfer function $F(s)$, the $\mathcal{H}_\infty$ norm of F is defined as

$$\|F(s)\|_\infty = \max_\omega |F(j\omega)| \ ,$$

which is simply the maximum gain of F over all frequencies. The constraints are then specified to limit $\|F\|_\infty$,

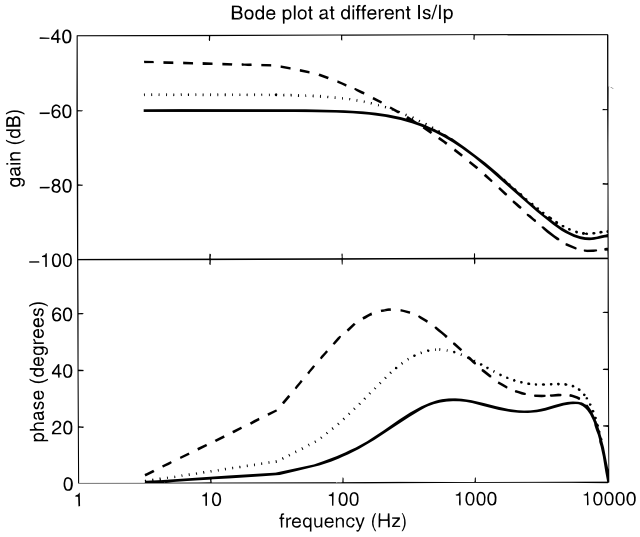

Fig. 4. Bode plot of plasma response at different elongations: $\kappa = 1.59$ (solid), 1.56 (dot), and 1.50 (dash).

where F is chosen to be a closed-loop transfer function multiplied by a frequency weight. If the loop gain $L(s)$ for the system in Fig. 5 is defined as

$$L(s) = P(s)C(s) \ ,$$

then the closed-loop sensitivity is $S(s) = 1/[1 + L(s)]$ and the complementary sensitivity is $T(s) = L(s)S(s)$. Three weighted bounds were used on T, CS, and S to specify robust stability margins, to reduce the effect of 600-Hz noise on the amplifier signals, and to limit the steady-state tracking error. The frequency-dependent weights were chosen in a heuristic manner to provide a good compromise among the three objectives. The choice of constraints and weights is described in turn.

Given a nominal model of a plant P and a controller C, it is possible that the nominal closed loop is stable but that a small variation or error in P causes the closed loop to become unstable. A robustly stabilizing controller is one for which closed-loop stability is guaranteed for the nominal plant and a specified range of plants. The first objective was to specify a robustly stabilizing controller. A set of plant models based on the nominal model P with multiplicative uncertainty bound (as in Fig. 5) can be considered

$$P' \in \{P(1 + W_1 \Delta); \|\Delta(s)\|_\infty < \gamma\} \ ,$$

where W_1 is a frequency weight and Δ can be any transfer function such that P and P' have the same number of unstable poles. The scalar γ is a bound on the size of the uncertainty for the set of plants P'.

A controller stabilizes any plant in the set P' if and only if

$$\|\gamma W_1 T\|_\infty < 1 \ . \qquad (1)$$

The weight W_1 was chosen to be a high-pass filter on the assumption that the plant model is relatively more uncertain at high frequencies. The high-frequency gain is a factor of 10 larger than the low-frequency gain. The filter time constants were chosen by examining stability margins indicated by Nyquist plots of the loop gain. The transfer function of W_1 is

$$W_1 = \frac{10\tau_1 s + 1}{\tau_1 s + 1} \ ,$$

where $\tau_1 = 50\ \mu$s. The amplitude spectrum of W_1 is plotted in Fig. 6. The value of γ is found from an optimization process that calculates the maximum value of γ and a controller for which the three constraints can be satisfied. Large values of γ indicate that a large range of plants can be stabilized, so γ can be considered as a measure of stability margin.

The closed-loop response v to noise n (Fig. 5) is CS. The effect of a 600-Hz noise source on v can be reduced by specifying the constraint

$$\|W_2 CS\|_\infty < 1 \ . \qquad (2)$$

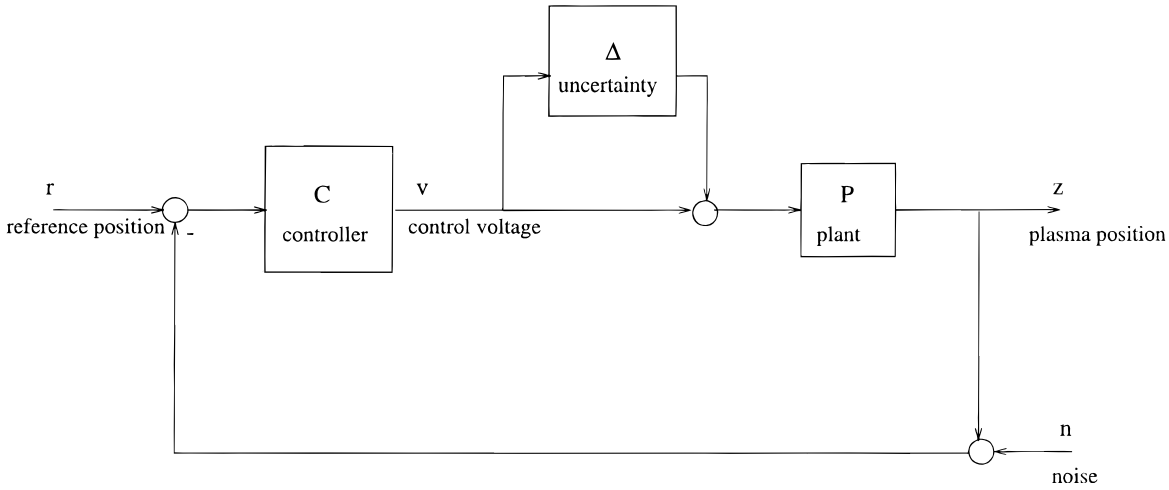

Fig. 5. Block diagram of control system including plant uncertainty model.

The weight W_2 is a bandpass filter with peak at 600 Hz (Fig. 6),

$$W_2 = \frac{1}{100} \times \frac{(s - z_2)(s - \bar{z}_2)}{(s - p_2)(s - \bar{p}_2)} \ ,$$

where $z_2 = (-317 + 3775j)\ \mathrm{s}^{-1}$, $p_2 = (-0.5 + 3768j)\ \mathrm{s}^{-1}$, and the overbar denotes complex conjugation. The high-frequency gain of W_2 ($\frac{1}{100}$) was chosen to limit the high-frequency gain of the controller to avoid amplifying high-frequency noise.

The transfer function from noise or disturbance to position error e is S and can be penalized with a third constraint

$$\|W_3 S\|_\infty < 1 \ . \tag{3}$$

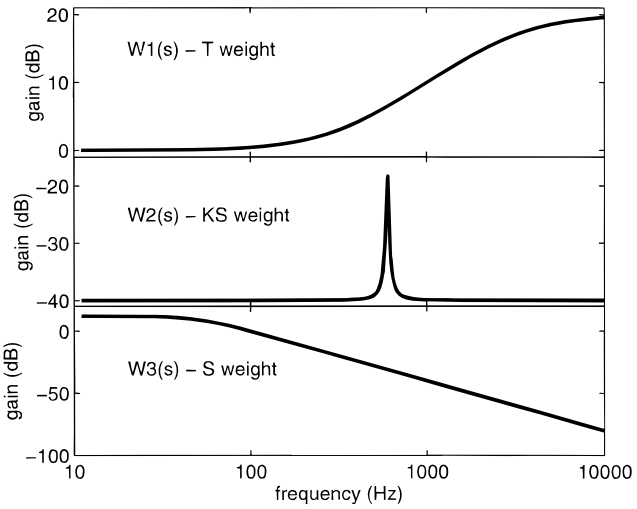

Fig. 6. Weights for $\mathcal{H}_\infty$ controller design.

If W_3 is large then S must be small to satisfy the constraint. Since the reference position signal is constant during the flattop period of a plasma shot, only low-frequency tracking is required. The filter W_3 was chosen to be a low-pass filter with cutoff at 50 Hz,

$$W_3 = \frac{3.948 \times 10^5}{(s - p_3)(s - \bar{p}_3)} \ ,$$

where $p_3 = (-222.1 - 222.1j)\ \mathrm{s}^{-1}$.

Given a model of the plant P and having chosen weights W_1, W_2, and W_3 for closed-loop stability and performance, the $\mathcal{H}_\infty$ optimal controller for COMPASS-D would satisfy the three constraints for the largest value of the stability margin γ. This controller is difficult to calculate, but a more tractable problem is to obtain a controller that maximizes γ subject to

$$\left\| \begin{matrix} \gamma W_1 T \\ W_2 CS \\ W_3 S \end{matrix} \right\|_\infty < 1 \Leftrightarrow \| (|\gamma W_1 T|^2 + |W_2 CS|^2 + |W_3 S|^2)^{1/2} \|_\infty < 1 \ . \tag{4}$$

Satisfying Eq. (4) implies that the three conditions in Eqs. (1), (2), and (3) are simultaneously satisfied.

The overall design approach was to choose the weights and use the Matlab Robust Control Toolbox[8] to obtain the $\mathcal{H}_\infty$ optimal controller $C(s)$ that satisfies Eq. (4). The resulting controller is ninth order (the combined order of the plant P and the weights W_1, W_2, and W_3). The resulting optimal stability margin is $\gamma = 0.238$. The Nyquist plot of the loop gain L in Fig. 7 is a polar plot of the frequency response of the loop gain L. For COMPASS-D, the plot must encircle the $-1 + 0j$ point once anticlockwise for closed-loop stability. For robust stability the gap between the loop gain and the $-1 + 0j$ must be large enough so that an anticlockwise encirclement can be maintained for changes in the frequency

response of the plant model. The D.C. gain of L is -5.19. This is relatively large so that the tracking error S is small. Increasing the penalty on the tracking error by making the D.C. gain of W_3 larger increases the magnitude of the resulting D.C. loop gain. At low frequencies the gain of L decreases with frequency, and the phase of L is <180 deg. At 180 Hz the loop gain crosses the real axis at $-1.5 + 0j$ and later crosses the axis again at 1650 Hz and $-0.357 + 0j$. Near the $-1 + 0j$ point, the phase of L is >180 deg, ensuring that there is one anticlockwise encirclement. The distance between the loop gain and the $-1 + 0j$ point is most directly affected by the weight γW_1. The weight W_1 was fixed and defined the relative level of uncertainty at high and low frequencies, and the distance was maximized by choosing the maximum value of γ for which a controller satisfied all three constraints. It was found that larger values of γ were achieved if the high-frequency gain of weight W_3 was made smaller.

There is a trade-off between robust stability margin and high-frequency noise amplification. The controller contains a notch at 600 Hz, and this causes the plot to pass close to the origin ($|L| \approx 0.14$ at 600 Hz). At frequencies above 1 kHz, the loop gain tends to the origin. The controller was checked with models of the plasma during startup to ensure stability at low elongation. The controller was then converted to discrete time form and finally tested on COMPASS-D.

The plot in Fig. 8 shows the result of testing the $\mathcal{H}_\infty$ controller on COMPASS-D for a plasma discharge where the elongation is slowly increased to $\kappa = 1.6$ and beyond. The 600-Hz component is rejected as required up to 195 ms. Beyond this time the system begins to resonate and finally becomes closed loop unstable. At the required operating point $\kappa = 1.6$, the system is stable but highly resonant. This is an improvement on a flux-loop-only P + D controller, but the resonance indicates that the stability margin of the system is poor. Further tuning of the model and controller weights is possible and has achieved the required performance.[5,9]

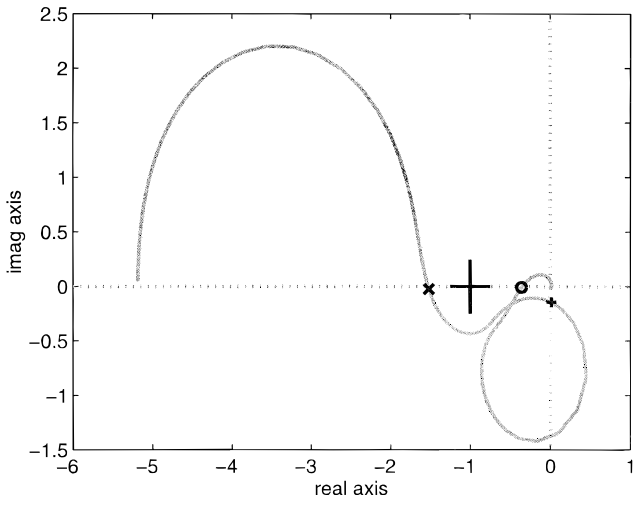

Fig. 7. Nyquist plot of loop gain $L(s)$ with the $\mathcal{H}_\infty$ controller. The D.C. gain is -5.19, and at 600 Hz the plot passes close to the origin. Points are marked at 180 (x), 600 (+), and 1650 Hz (o).

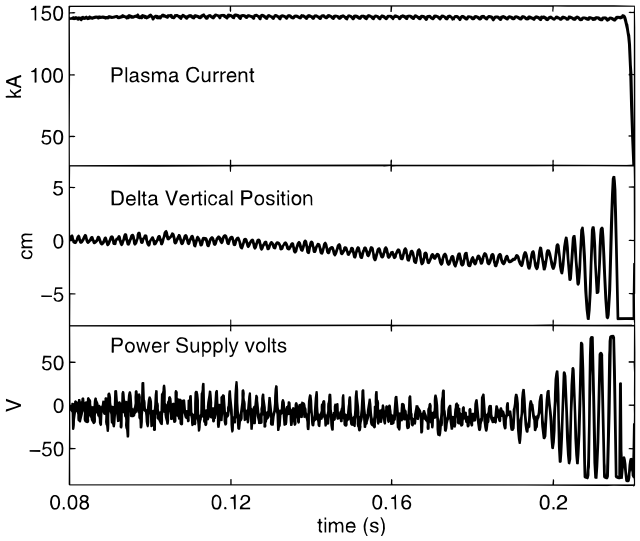

Fig. 8. Position and amplifier response for the $\mathcal{H}_\infty$ controller. The plasma elongation slowly increases through the shot (#15946).

The results demonstrate that high-order controllers can have advantages over simple P + D controllers. It has been shown on COMPASS-D how a high-order controller can be used to improve the stability properties of the vertical position loop and to reduce the effect of noise on amplifier output signals.

ELM AND IMPULSE RESPONSE

Edge-localized modes of different types are often observed on COMPASS-D. Large, separated ELMs cause the largest excursions in the plasma position and demand large voltages from the control amplifiers. Figure 9 shows a typical amplifier input and flux loop position response to large, separated ELMs, with the current P + D controller. Each spike in the D_α signal corresponds to an ELM. Each ELM causes an impulselike response excursion in the plasma position (up to ~2 mm peak to peak) and large voltage and current swings from the control amplifier (up to ~60 V and ~300 A peak to peak). Occasionally the amplifiers saturate, leading to loss of stability.

Minimizing the peak response to an ELM is a useful objective, and one way this can be achieved is to model ELMs as impulse disturbances and minimize the peak of the impulse response of the system. In this section we find a theoretically optimal controller that minimizes the peak of the impulse response.

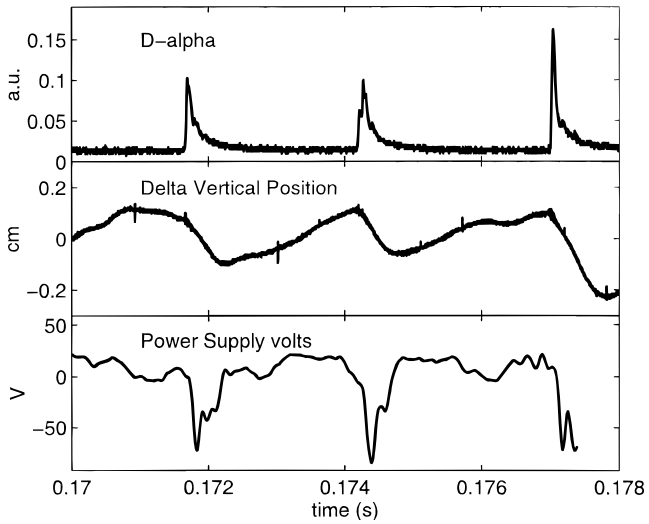

Fig. 9. D_α, flux loop position error signal, and amplifier output during large separated ELMs (#14787).

Dahleh and Pearson[2] developed a method for deriving the discrete time optimal controller that minimized the maximum magnitude of the response for a fixed input. For an arbitrary plant, the optimal response is found from the solution of a linear programming problem with a finite number of variables and a constraint involving the sum of a series of an infinite number of terms. The resulting optimal controller is of infinite order. A restricted-order optimal controller can be found if the series is truncated. We show herein that for a restricted class of plants (which includes the COMPASS-D model), the linear programming problem can be solved analytically.

In this section the Z-transform of a time-sequence f_i is defined as in Ref. 2:

$$F(z) = \sum_{i=0}^{\infty} f_i z^i \ .$$

Note that this is defined in terms of the complex variable z and not the more usual z^{-1}. Using the preceding definition, $F(z)$ is unstable if it has any poles inside the unit disk of the z-plane. Also if $F(z)$ represents a plant model with an m sample time delay, then $F(z)$ has m zeros at the origin. Letting t_i represent the impulse response of the closed-loop transfer function $T(z) = P(z)C(z)[1 + P(z)C(z)]^{-1}$ and defining the peak of the impulse response $\|t_i\|_\infty = \max_i |t_i|$, then the optimal cost is

$$\mu_* = \min\{\|t_i\|_\infty : C \text{ stabilizes } P\} \ .$$

COMPASS-D has a single unstable pole. Tustin's approximation can be used to find the relationship between the continuous time pole p in the s-plane and the discrete time pole a in the z-plane,

$$a = \frac{2f_s - p}{2f_s + p} \ ,$$

where f_s is the sampling frequency. The COMPASS-D model $[P(s)]$ used in the previous section has the unstable pole at $p = 2260\ \text{s}^{-1}$. For a sampling frequency $f_s = 20$ kHz, the discrete time pole is $a = 0.893$. The discrete time equivalent of $P(s)$ also has two zeros at the origin (i.e., $m = 2$) because of the sample delay in the discrete time equivalent of P_{FL} and one sample delay from the discrete time approximation of P_c. We now give the result for COMPASS-D–type plants:

Proposition 1: Consider a plant with a single unstable pole at a, m zeros at the origin, and no other poles or zeros inside the unit disk.

a. The optimal cost is

$$\mu_* = \frac{1 - |a|}{|a|^m} \ .$$

The optimal closed-loop response is a step of height μ_* after a time delay of m samples as shown in Fig. 10. The order of the controller is infinite.

b. Consider the case when the order of the closed-loop response is restricted to n, where $n \geq n_n + n_d + 1$ and n_n and n_d are the orders of the plant numerator and denominator, respectively. Then the restricted order optimal cost is

$$\mu_n = \frac{1 - |a|}{|a|^m - |a|^{n+1}} \ .$$

The resulting response is a pulse as shown in Fig. 10. The controller order is $n_d + n - m - 1$.

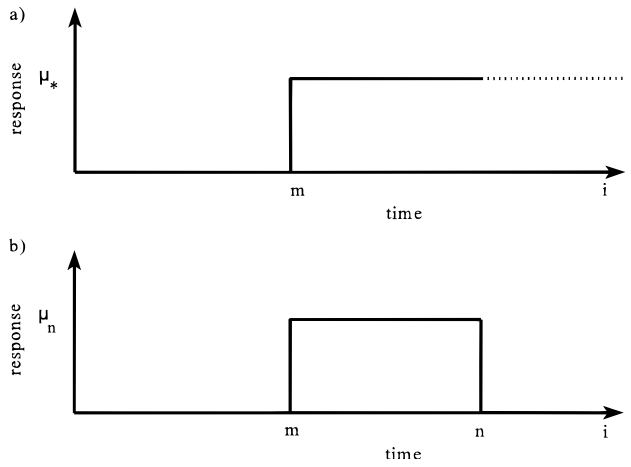

Fig. 10. (a) Plot of optimal impulse response and (b) optimal restricted order response.

Note that the performance does not depend on any stable poles or any zeros outside the unit disk in the plant; these are canceled by the controller. The proofs are provided in Ref. 5 and involve formulating and solving the linear programming problem to find the optimal stabilizing controller. The controller can be synthesized by deconvolution of the closed-loop transfer function.

Figure 11 contains plots of μ_* against a for different values of m. It shows clearly that the optimal peak response increases as the time constant of the unstable pole decreases. For COMPASS-D this implies that the optimal performance is worse for plasmas with higher elongations. It also shows that the optimal cost increases with m. The plot of μ_n against n (Fig. 12) shows that allowing the order of the response to increase improves the performance of the controller. In summary, there is a tradeoff among the time to settle, the open-loop growth rate of the plant, and the maximum magnitude of the impulse response of the system.

Improving the impulse response is expected to improve the ELM response. The results provided here allow the potential for improvement to be judged. The COMPASS-D P + D controller (using flux loop and IPR signals) has a theoretical peak response of 0.173 to a unit pulse of width 50 μs. The impulse response of the $\mathcal{H}_\infty$ controller designed using the weights in Eqs. (1), (2), and (3) has a peak of 0.254 and so would be expected to require larger voltages in the presence of ELMs. The theoretical optimal performance is 0.135, which indicates that the P + D system performance is reasonably good in this respect. If we require the settling time of the impulse response to be limited to, for example, 1 ms, then the restricted order optimal cost is 0.15, and the optimal controller order is 21.

Of course, it is not suggested that an actual peak optimal controller is used on COMPASS-D because it would not address the requirements for stability margin or 600-Hz noise rejection. Nevertheless, the information provided is valuable because it sets the limits of performance of the system against which controllers can be evaluated.

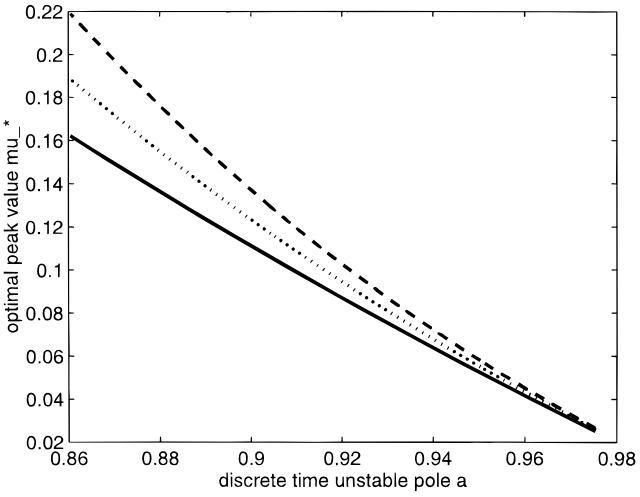

Fig. 11. Plot of μ_* against a for $m = 1$ (solid), 2 (dot), and 3 (dash).

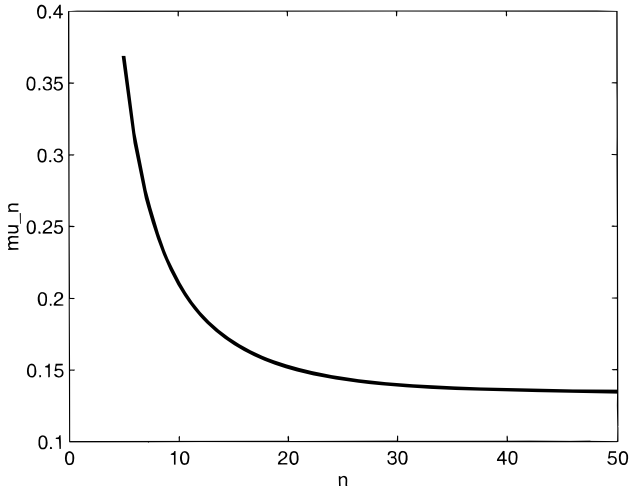

Fig. 12. Plot of μ_n against n for $a = 0.893$, $m = 2$.

CONCLUSIONS

The current analog P + D control system is satisfactory in many respects but is not designed to reduce the level of 600-Hz noise in the system and is unable to stabilize the plasma vertical position using only external measurements of position. High-order controllers offer more flexibility but can be more difficult to design. It has been shown that $\mathcal{H}_\infty$ theory can be used to address the stability and 600-Hz noise problems, and an $\mathcal{H}_\infty$ controller has been implemented on a DSP and tested on COMPASS-D. The results are encouraging in that the high-order $\mathcal{H}_\infty$ controller was able to stabilize the plasma at the required operating point and attenuate the 600-Hz noise at lower elongations. Neither of these is possible with a simple P + D controller.

Large, separated ELMs on COMPASS-D cause impulselike responses to be observed, and it is expected that minimizing the peak impulse response of the system would reduce the voltage requirement to accommodate ELM disturbances. A method exists for finding the optimal controller[2] and can be simplified for the COMPASS-D case. The results would be useful when designing any multiobjective controller since they specify the limits of performance in the presence of ELMs that any controller could achieve.

ACKNOWLEDGMENTS

This work is jointly funded by the U.K. Department of Trade and Industry, Euratom, and the U.K. Engineering and

Physical Sciences Research Council (CASE award and grant GR/J06078). The authors would also like to thank the COMPASS-D team for assistance with the experimental work.

REFERENCES

1. J. C. DOYLE, B. A. FRANCIS, and A. R. TANNENBAUM, *Feedback Control Theory*, Macmillan, New York (1992).

2. M. A. DAHLEH and J. B. PEARSON, "Minimization of a Regulated Response to a Fixed Input," *IEEE Trans. Automat. Control*, **33**, *10*, 924 (Oct. 1988).

3. J. A. BOOTH, R. T. CROSSLAND, R. J. HAYWARD, P. KEOGH, and A. P. PRATT, "COMPASS Magnetic Field Coils and Structure Systems," *Proc. 14th Symp. Fusion Technology*, September 8–12, 1986, Avignon, France, Vol. 2, p. 1781 (1986).

4. P. VYAS, A. W. MORRIS, and D. MUSTAFA, "Analysis of Experimental Performance and Robust Stability on the COMPASS-D Tokamak," *Proc. 18th Symp. Fusion Technology*, August 22–26, 1994, Karlsruhe, Germany, Vol. 1, p. 703 (1995).

5. P. VYAS, "Plasma Vertical Position Control in the COMPASS-D Tokamak," DPhil Thesis, University of Oxford, United Kingdom (1996).

6. M. M. M. AL-HUSARI et al., "Vertical Stabilisation of Tokamak Plasmas," *Proc. 30th IEEE Conf. Decision and Control*, December 1991, Brighton, England, p. 1165 (1991).

7. A. PORTONE, "Controllability of NET Plasmas After Loss of Beta Events," *Proc. 17th Symp. Fusion Technology*, September 14–18, 1992, Rome, Italy, Vol. 1, p. 623 (1992).

8. R. Y. CHIANG and M. G. SAFONOV, *Robust Control Toolbox User's Guide*, The Mathworks Inc., Natick, Massachusetts (1988).

9. J. R. GOSSNER, P. VYAS, and B. KOUVARITAKIS, "Application of Cautious Stable Predictive Control to Vertical Positioning in COMPASS-D," Oxford University technical report OUEL 2092/96, submitted to *IEEE Trans. Control Systems Technology* (1996).

Parag Vyas (BEng, electrical and electronic engineering, Imperial College, London, United Kingdom, 1992; DPhil, University of Oxford, United Kingdom, 1996) is a research engineer at the Centre de Recherches en Physique des Plasmas, Ecole Polytechnique Fédéral de Lausanne, Switzerland. As a graduate student he investigated the plasma vertical position control system on the COMPASS-D tokamak. His research interests include the modeling and control of plasma shape and position in the Tokamak Configuration Variable (TCV) and International Thermonuclear Experimental Reactor (ITER) tokamaks.

Denis Mustafa [BA (Hons), engineering science, University of Oxford, United Kingdom, 1986; PhD, robust control theory, University of Cambridge, United Kingdom, 1989] is a derivatives modeler at JP Morgan. His research interests are in robust and optimal control.

William Morris [BA (Hons), physics, Merton College Oxford, United Kingdom, 1980; MSc, science and applications of electric plasmas, University of Oxford, United Kingdom, 1981; DPhil, large-scale instabilities in tokamaks, University of Oxford] conducts tokamak research for fusion at UKAEA Fusion, Culham Science Centre. His research interests lie in all aspects of experimental physics of magnetic confinement for fusion, with an emphasis on plasma instabilities.